**Part of Topical Section on
Recent Advances in Diamond Science and Technology**

physica **pssa** status solidi

www.pss-a.com

applications and materials science

The effect of molecular structure of organic compound on the direct high-pressure synthesis of boron-doped nanodiamond

Evgeny A. Ekimov*,1, Oleg S. Kudryavtsev2, Stuart Turner3, Svetlana Korneychuk3, Vladimir P. Sirotinkin4, Tatiana A. Dolenko5,6, Alexey M. Vervald5, and Igor I. Vlasov2,6

[1] Institute for High Pressure Physics, Russian Academy of Sciences, Moscow, 142190 Troitsk, Russia
[2] General Physics Institute, Russian Academy of Sciences, Vavilov Str. 38, 119991 Moscow, Russia
[3] EMAT, University of Antwerp, Groenenborgerlaan 171, 2020 Antwerp, Belgium
[4] Baikov Institute of Metallurgy and Materials Science, Russian Academy of Sciences, Leninskii pr. 49, 119991 Moscow, Russia
[5] Moscow State University, Leninskie Gory 1/2, 119991 Moscow, Russia
[6] National Research Nuclear University MEPhI, Kashirskoe Road 31, 115409 Moscow, Russia

Evolution of crystalline phases with temperature has been studied in materials produced by high-pressure high-temperature treatment of 9-borabicyclo[3.3.1]nonane dimer (9BBN), triphenylborane and trimesitylborane. The boron-doped diamond nanoparticles with a size below 10 nm were obtained at 8–9 GPa and temperatures 970–1250 °C from 9BBN only. Bridged structure and the presence of boron atom in the carbon cycle of 9BBN were revealed to be a key point for the direct synthesis of doped diamond nanocrystals. The diffusional transformation of the disordered carbon phase is suggested to be the main mechanism of the nanodiamond formation from 9BBN in the temperature range of 970–1400 °C. Aqueous suspensions of primary boron-doped diamond nanocrystals were prepared upon removal of non-diamond phases that opens wide opportunities for application of this new nanomaterial in electronics and biotechnologies.

1 Introduction High-pressure synthesis of nanodiamonds from organic compounds, reported by Wentorf half a century ago [1], is now becoming extremely high demanded for obtaining nanocrystals of diamond with optically and electrically active impurities. Nanodiamonds doped with optically and electrically active impurities promise attractive applications in biology, magnetometry, nanoscopy, and in different modern quantum information processing and communication technologies [2–7]. Nano- and microcrystalline diamonds with Si–V, N–V, and Ge–V defects have been recently synthesized from naphthalene-based mixtures of reagents at pressures of 8–9 GPa [8, 9]. Although the portion of diamond nanocrystals in the samples obtained was negligible (∼5%), their structural quality was almost the same as for bulk diamond [9, 10]. In contrast to the synthesis of diamond from naphthalene with planar molecule structure, decomposition of an individual compound with a bridged structure and boron atom in the carbon 9BBN cycle proceeds forming only a nanodiamond component with a boron impurity in the diamond lattice [11]. Despite recent advances in the direct synthesis of nanodiamonds under pressures, the questions of the mechanism of nanodiamond formation from organic compounds below the direct conversion of graphite into diamond (10–11 GPa [12, 13]) and of impurity doping of nanodiamond, remain unanswered to date. In the few studies on the synthesis of nanodiamonds from organic compounds, the key role of the structure of the starting compounds in the formation of diamond nuclei has been suggested [1, 14, 15]. According to this suggestion, the structures of saturated

hydrocarbons (paraffin, polyethylene) and of cyclic compounds with carbon bridges and with sp^3-hybridized carbon atoms (adamantane, camphene), contribute to the formation of nanodiamond, while the planar structure of the aromatic compounds (naphthalene, anthracene) induces the formation of a perfect graphite, which hinders the further formation of the diamond. Favorable atomic ratio of H/C (1.6–0.03) in the initial hydrocarbons has been proposed also as a condition of the nanodiamond formation [15]. Besides the influence of hydrogen on the diamond formation from organic compounds, it was noted that the noticeable presence of nitrogen in the structure of organic compounds is favorable for the graphite formation and adverse for the diamond synthesis. The role of oxygen has not been revealed, but its presence does not block the diamond formation process [1].

Recently, the production of diamond nano- and microcrystals from naphthalene and fluorinated graphite mixtures was associated with formation, at the intermediate stage of transformation, of onion-like and micro-sized flacked graphite, whose sizes are inherited by the diamond [16]. It should be noted that the idea of a key role of nanographite in the nanodiamond synthesis was stated earlier in the study of the behavior of individual organic compounds [15], as well as of carbon materials [17] under high pressure. The latter case concerns the synthesis of nanodiamonds at pressures higher than the pressure of direct graphite-to-diamond transformation. In general, there are many contradictions in the literature data regarding the behavior of the same organic compounds at high pressures and temperatures. Thereupon, the systematic studies of regularities of high-pressure decomposition of individual organic compounds containing atoms of doping elements, as well as the study of the structure and composition of the produced carbon materials are still required.

The aim of present work was to study the effect of structure of boron-containing organic compounds on phase transformations under pressure and the establishment of formation regularities for boron-doped nanodiamonds.

2 Methods The following organic compounds were used in the study: 9-borabicyclo [3.3.1] nonane dimer, (9BBN, $C_{16}H_{30}B_2$), triphenylborane ($C_{18}H_{15}B$), and trimesitylborane ($C_{27}H_{33}B$). The carbon skeleton of the 9BBN molecule with sp^3-hybridized carbon, in fact, is a building block of the diamond lattice, where boron is a part of the carbon cycle. On the contrary, the triphenylborane and trimesitylborane compounds contain plane carbon cycles of sp^2-hybridized carbon interconnected by boron atom that favor the formation of a graphite structure. Toroid-type high-pressure chamber with graphite capsules were used for the sample preparation [18]. The capsules were filled with starting materials in an atmosphere of high purity argon. Experiments were carried out at pressure 8–9 GPa and at temperatures ranging from 600 to 1700 °C. The exposure time at constant P and T was 1–2 min. The capsules were placed in a container (made of $CaCO_3$), in the sleeves

(made of sintered ZrO_2) separating the capsule from the container. The butt-ends of the capsule were isolated with molybdenum disks of 0.3 mm thick from the surface of hard-alloyed cameras. The temperature was determined by a chromel-alumel or a platinum-rhodium thermocouple PR 30/6. Determination of elemental composition of the samples and of their various sections, as well as the study of morphology of the synthesis products, was carried out using an electron microscope JEOL JSM-6390LV with the EDS module for microanalysis. In order to determine the phase composition of the samples, an X-ray diffractometer «Ultima IV» by «Rigaku» (Cu Kα radiation, Ni filter) was used.

Transmission electron microscopy investigations of samples were performed with use of electron microscopes: JEOL 3000 F at 300 kV, cubed FEI Titan at 120 kV, and FEI Osiris at 200 kV. EELS data were taken in a cubed FEI Titan transmission electron microscope equipped with Gatan electron spectrometer.

The synthesized samples were purified from non-diamond phases in a boiling mixture of concentrated nitric/sulfuric (1:3) acids. Then the acids were washed out with bidistilled water in the process of seven washing/centrifugation cycles for 20 min (Centrifuge LMC-3000, BioSan, $1700 \times g$). The resulting precipitate was studied using confocal Raman spectroscopy.

The size of nanodiamond particles was measured in water suspensions by the method of dynamic light scattering (DLS) (analyzer ALV-CGS-5000/6010 Langen, Germany). The concentration of nanodiamond in the water suspension was $0.5\,\mathrm{g\,L^{-1}}$. Deionized bidistilled water with specific electrical conductivity $0.1\,\mu\mathrm{S\,cm^{-1}}$ was used in the sample preparation.

3 Results and discussion
3.1 Phase and structural transformations Typical morphologies for samples, obtained by thermobaric treatment of 9BBN, are shown in Fig. 1. Initially, 9BBN is a substance of white transparent crystals which are easily oxidized and adsorb water in air. At the synthesis temperatures up to 650 °C, the 9BBN transforms into a glassy transparent material of amber color which is substantially more stable under the conditions of the air atmosphere. With further temperature increase, a matte-black sooty product indicating decomposition of the organic matter is formed. At the synthesis temperatures above 1600 °C, the formation of the diamond crystals of two fractions with dimensions of about 1 and 0.1–0.3 μm is observed in the samples by scanning electron microscopy.

X-ray phase analysis and Raman spectroscopy investigations showed that the "amber" substance has amorphous structure, while for the "sooty" product, obtained at 800 °C, the presence of three broad lines at angles 26° (graphite), 44° (graphite + diamond), and 77° (graphite) were observed on the X-ray diffraction patterns (Fig. 2). Significant broadening of the diffraction lines indicates nanocrystalline nature of the phases, yet, the presence of an amorphous component is not excluded. Two diamond peaks are observed in the
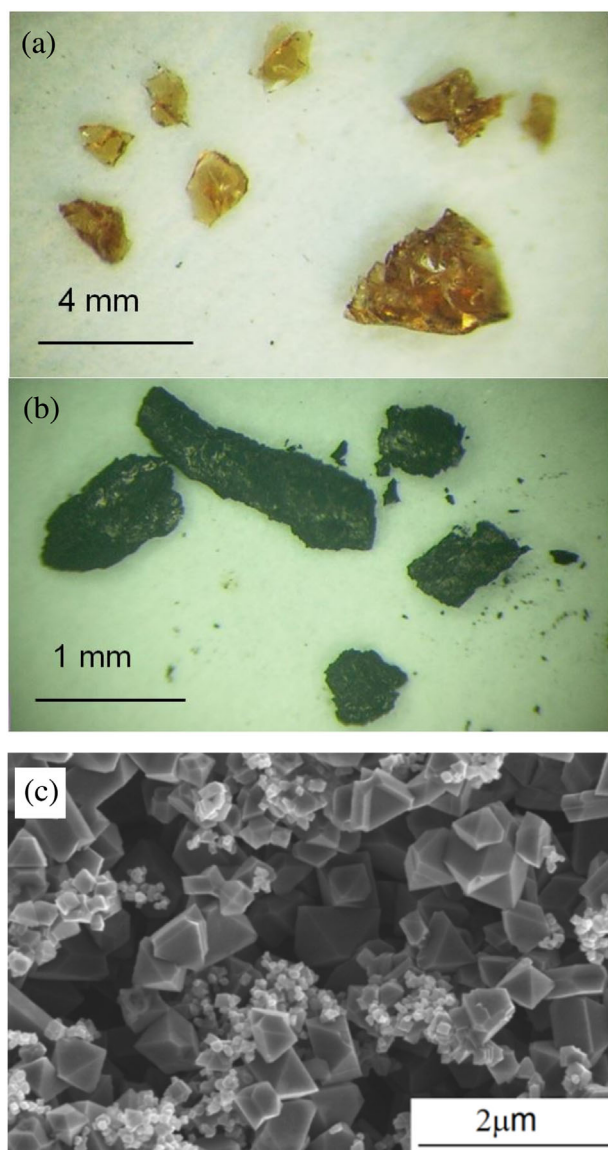
Figure 1 Morphology of the synthesis products obtained by thermobaric 9BBN treatment: (a) amorphous substance (650 °C), (b) sooty product (800 °C), (c) submicron and micron-sized crystals of diamond and boron carbide (1600 °C).

diffraction patterns of the samples synthesized at temperatures of 970 °C. Three diamond peaks, in turn, are surely detected by X-rays in the samples synthesized at a temperature of about 1070 °C. Crystallite size of diamond was estimated by Selyakov–Scherrer's formula to be under 10 nm for the samples synthesized at temperatures below 1250 °C. The presence of a narrow line on the dome of a broad line (002) of graphite is due to hit of particles of graphite capsule into the analyzed material. This line is no longer being discussed in the work. For the samples synthesized in the temperature range 800–1250 °C, the thickness L_c of graphite crystallites, calculated from the half width of the graphite line (002), gives a value of about 2 nm.
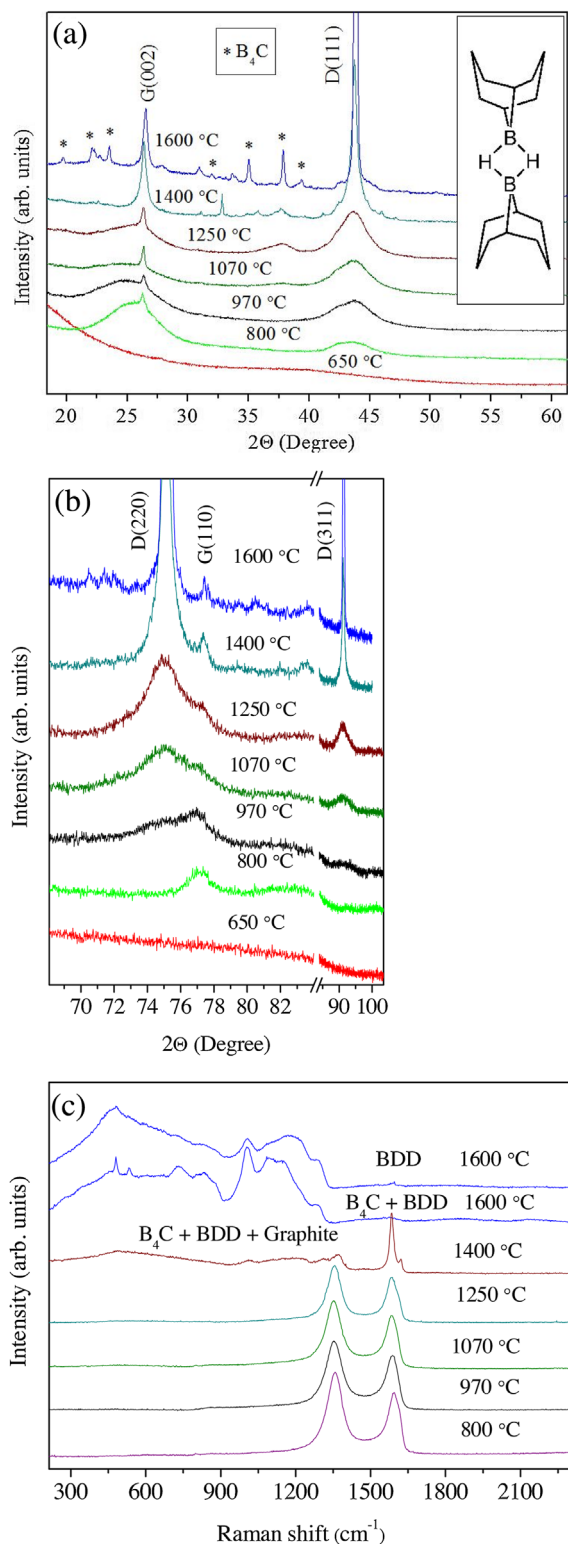

Figure 2 Phase transformations of 9BBN in the temperature range 650–1600 °C under pressure 8–9 GPa: (a, b) X-ray phase analysis, (c) Raman spectroscopy: BDD, boron-doped diamond; D, diamond; G, graphite; the two upper spectra relate to the same sample shown in Fig. 1c.

Raman spectra of these samples are practically identical: two wide lines D ($1356 \, \text{cm}^{-1}$) and G ($1585–1590 \, \text{cm}^{-1}$) are present; the lateral size L_a of graphite crystallite estimated by the ratio $I\,(G)/I\,(D)$ [19] is 3–4 nm.

As evidenced by X-ray phase analysis and Raman spectroscopy data, the samples synthesized at temperatures above 1400 °C contain well-structured graphite, diamond, and boron carbide. Boron in oxidized form was also detected in some of the samples. The Raman starts to detect diamond (Fig. 2c) in the samples synthesized at 1400 °C and higher. One can suggest that nanographite matrix material in the samples prepared at lower temperatures prevent the diamond identification by this method: the effective cross section of graphite in visible Raman is 50 times higher than that of diamond. Down-shifted diamond line at $1310 \, \text{cm}^{-1}$ and local phonon modes at 500, 1000, and $1200 \, \text{cm}^{-1}$, typical for heavily boron-doped diamond [20], are observed in spectra of samples synthesized at 1600 and 1400 °C. Narrow peaks at 480 and $530 \, \text{cm}^{-1}$, and broad 700, 820, 1000, 1100, and $1130 \, \text{cm}^{-1}$ bands, characteristic of boron carbide B_4C synthesized at high pressures [21], are detected in spectra of samples obtained at 1600 °C.

Studying the behavior of compounds with planar carbon cycles (triphenylborane, $C_{18}H_{15}B$ and trimesitylborane, $C_{27}H_{33}B$), in which boron atoms are not part of the carbon cycle, showed that the formation of nanodiamond does not occur in the range of temperatures up to 1400 °C. Figure 3 depicts typical stages in the evolution of the phase composition and structure of the trimesitylborane, $C_{27}H_{33}B$ compound. There are no principle differences in the decomposition behavior between triphenylborane and trimesitylborane substances, except the appearance of the oxidized forms of boron in the latter case due to the presence of water in the starting material. The formation of the graphite phase at decomposition of compounds with planar carbon cycles goes by a different scenario than for 9BBN. Its characteristic feature is more intense structuring under heating: with the temperature increase, the diffraction lines of graphite become noticeably narrower in diffraction patterns; diffraction reflections with indices (100), (004), (112), and others are more clearly recorded (Fig. 3a). Moreover, the changes in the relative intensities of the lines G and D and the appearance of a fine structure of the G-line with increasing temperature (Fig. 3b) indicate a higher ordering of a graphite-like phase for the same P–T conditions of the sample synthesis. The evaluation of the parameters L_c and L_a allows us to associate the observed changes in the Raman spectra and the X-ray diffraction data with the increase of the graphite crystallite size from 3 to 45 nm and from 3 to 5 nm, respectively, with the temperature increase in the range 800–1250 °C. Usually lateral size of a graphite crystallite is larger than its thickness. In our case, the smaller lateral size L_a of graphite crystallite can be associated with curvature of graphene packages under pressure.

The comparative analysis of the behavior of organic compounds with different structure shows that the planar
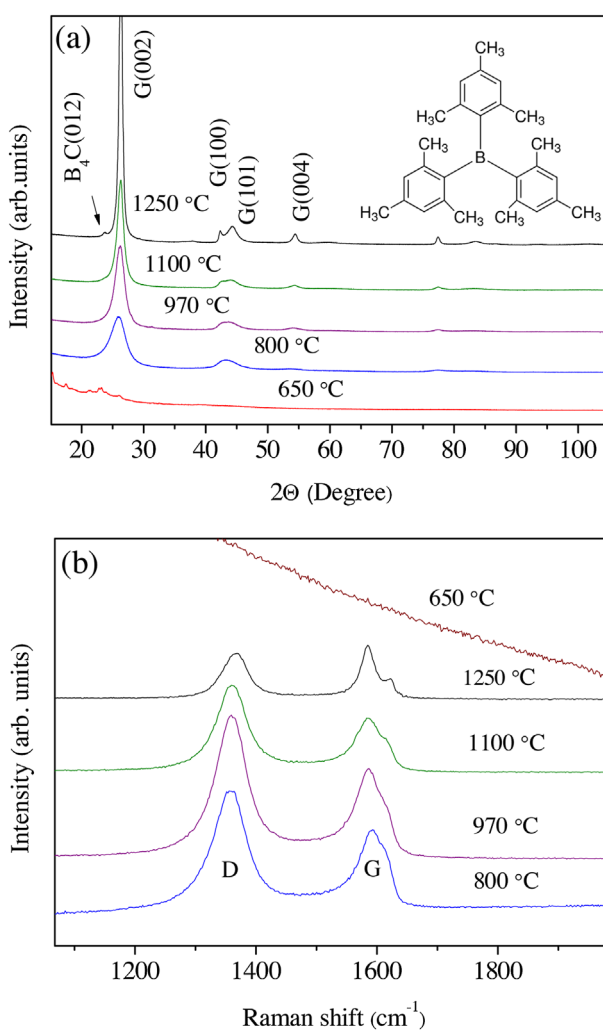

Figure 3 Evolution of phase composition of trimesitylborane compound ($C_{27}H_{33}B$) in the temperature range 650–1250 °C at pressure 8–9 GPa: (a) X-ray diffraction patterns, (b) Raman spectra.

structure of the carbon cycles induces a sequential transformation into graphite when heated under pressure.

At the temperature of 1250 °C, the samples from trimesitylborane represent well crystallized graphite, whereas in the samples synthesized from the 9BBN, graphite phase is present in a turbostratic nanocrystalline state. Thus, from the one hand, it can be assumed that the boron atom of the 9BBN molecule inhibits the formation of graphene layers at dehydrogenation. On the other hand, the original bridge-like skeleton structure of the sp3-hybridized carbon in the 9BBN molecule presenting a fragment of the diamond lattice promotes the formation of the diamond nuclei. It is worth noting that B–H and B–H–B bonds survive at pressure 8–9 GPa up to temperatures of 1100–1200 °C [22, 23]. If it happens in our case, then hydrogen can stabilize sp3-hybridization of boron in 9BBN and stimulate not only diamond nucleation, but also incorporation of boron into the diamond lattice. At synthesis

temperatures above 1400–1600 °C, well-faceted submicro- and micro-crystals of the diamond are mainly present in the samples that evidences the change in the diamond growth mechanism. It is known from the literature [24–28] that many non-metallic carbon solvents, including those, based on the system C–H–O [25, 27, 28], become catalysts of graphite-to-diamond transformation at a pressure of about 8 GPa and at temperatures above 1400–1600 °C. For these systems, dissolution of graphite and crystallization of diamond from the growth medium underlie the mechanism of diamond synthesis. High diffusion mobility of carbon atoms in the gas (liquid) growth medium at the synthesis temperatures causes rapid growth of micron-sized diamond crystals.

3.2 Transmission electron microscopy The microstructure of the samples, obtained by decomposition of 9BBN, was studied by transmission electron microscopy. It is found that nanodiamonds with an average size of about 5 nm are mainly formed in the samples at the synthesis temperatures of 970–1250 °C (Figs. 4 and 5). Besides the diamond, phases of strongly disordered carbon material and of nanographite are present in the samples in significant quantities. In electron diffraction patterns of samples, synthesized at 1070–1250 °C, a reflection at 2.4 Å is also observed meaning the presence of one more phase. The presence of this phase in the samples was also detected on X-ray diffraction patterns by the appearance of a broad peak at angles of 35–40°, but the nature of this phase was not clear. The study of individual nanoparticles by EELS proves that the phase with reflection at 2.4 Å is, in fact, crystalline boron carbide with composition close to $BC_{0.37}$. Thickness of graphene stacks in graphite nanoparticles agrees very well to the calculated parameter L_c, while parameter L_a corresponds to linear fragments of curved graphite flakes of about 15 nm long. For the sample synthesized at 1400 °C (Fig. 6), the size of the nanodiamonds differs significantly from particle to particle. There are big particles with the sizes around 30–50 nm and small particles with a diameter below 5 nm. Besides nanodiamonds, graphitic flakes are omnipresent. It is obvious that the synthesis temperatures 1250–1400 °C becomes border at which changes in the structure and morphology of the resulting phases take place. In contrast to the data published by us earlier [11], the synthesis of the samples in this work was made not in metal, but in a graphite capsule. Fundamental differences in the behavior of 9BBN by heating under pressure were not revealed, more indicating the role of the structure of the compound in the formation of nanodiamond than the conditions of hydrogen removal from the growth system [29].

3.3 The mechanism of the nanodiamond synthesis Nanodiamond particles in the sample, synthesized at 970 °C, are usually surrounded by an extensive phase of highly disordered carbon (Fig. 4b). After examining the sample, we have found no evidence that
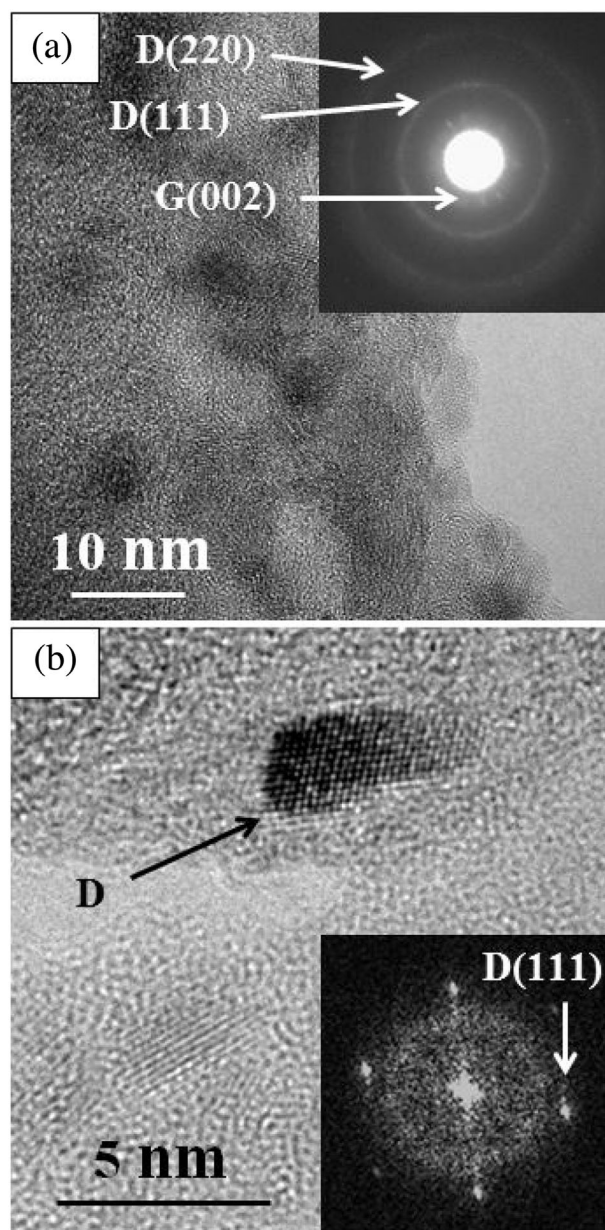

Figure 4 Microstructures (a, b) and electron diffraction patterns (inserts) of the samples synthesized from 9BBN at 970 °C. "D" in (b) denotes a nanodiamond particle.

the formation of the diamond nanoparticles is genetically (see Ref. [16]) associated with the appearance of the graphite nanoparticles. With the increase of the temperature, the structure of the samples also changes (Fig. 5). Surrounded by disordered carbon, one of the sides of the diamond crystals is usually contacted with a graphite crystallite, so that the planes (111) of the diamond and (002) of the graphite layers are parallel. At the same time, the diamonds do not penetrate into the graphite layers but grow in the disordered carbon phase. This fact points to the mechanism of heterogeneous formation of the diamond nuclei on graphene substrate. In general, the absence of a
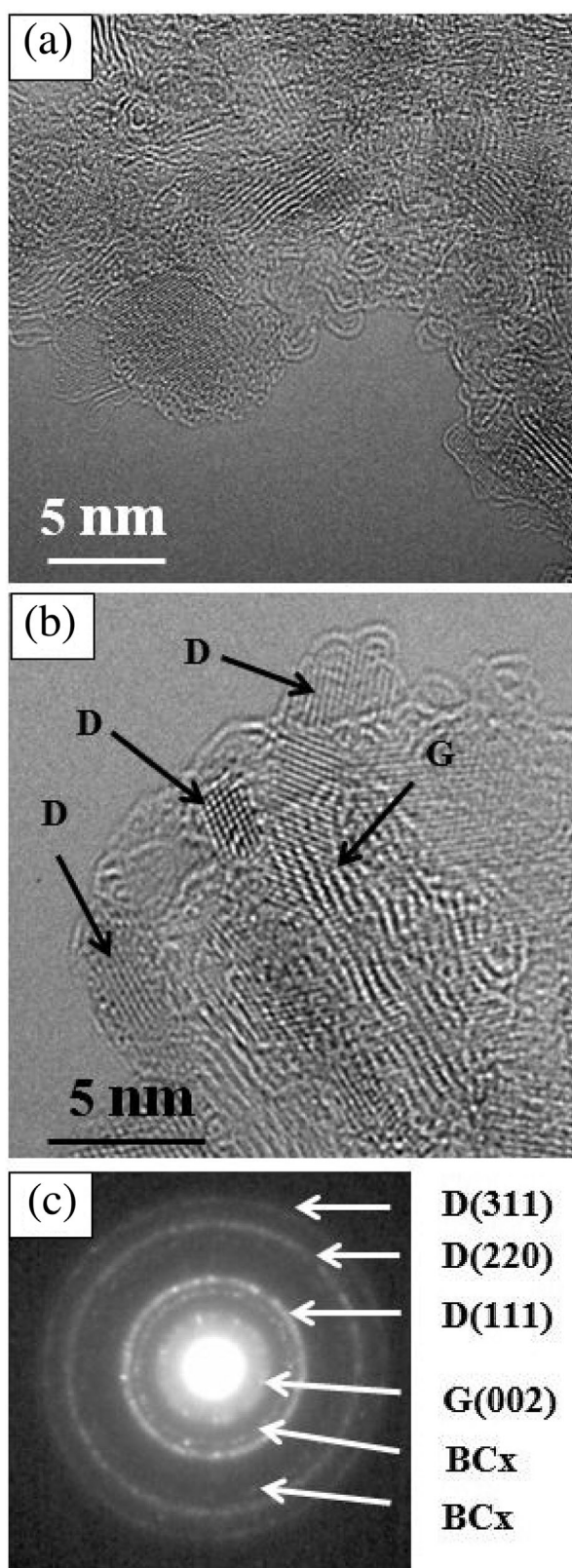
Figure 6 Microstructure (a) and electron diffraction pattern (b) of the samples synthesized from 9BBN at 1400 °C.

Figure 5 Microstructures (a, b) and electron diffraction pattern (c) of the samples synthesized from 9BBN at 1250 °C: Nanodiamonds, nanocrystalline graphite, and strongly disordered carbon material are clearly seen in (a, b).
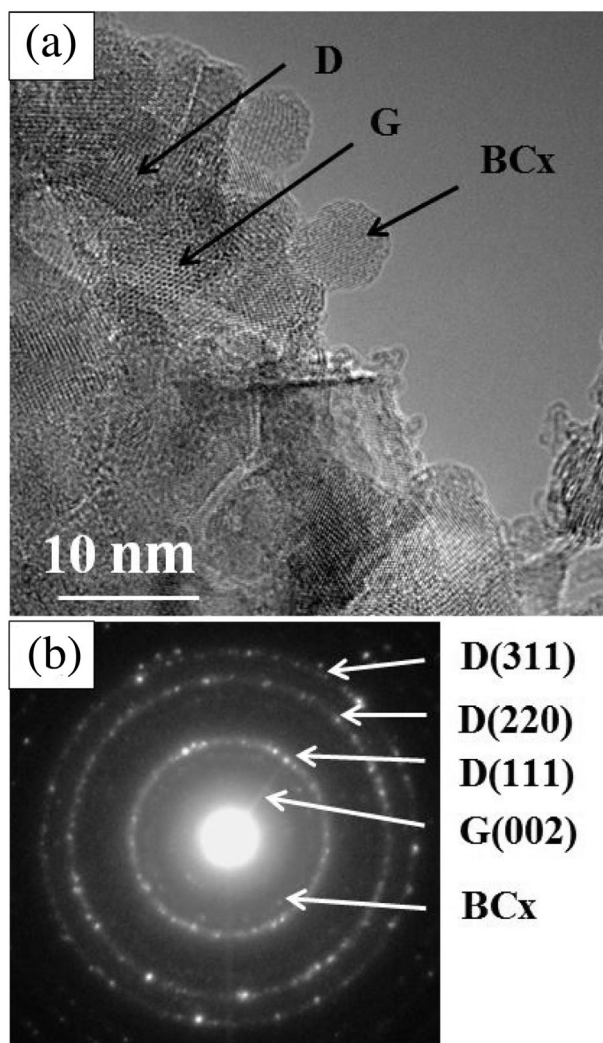
hexagonal "diamond" and of numerous stacking faults in the diamond crystals indicates the diffusional mechanism of nucleation and growth of the diamond crystals.

On the one hand, the martensitic transition requires quite perfect graphite structure and higher synthesis pressures causing integration of the diamond structure inside the graphite layers. On the other hand, the low temperatures at which the synthesis of the diamond is observed (∼970–1400 °C) do the solid-phase diffusional graphite-to-diamond transformation unlikely. Thus, the diffusion transformation of the strongly disordered carbon phase is regarded as the most probable mechanism of the diamond formation at synthesis temperatures below 1400 °C.

This mechanism has previously been proposed to explain the formation of nanodiamonds from disordered carbon under pressure of 15 GPa and at temperatures of about 1500 °C [17]. Our experiments indicate that this mechanism is also realized at lower P–T parameters, namely
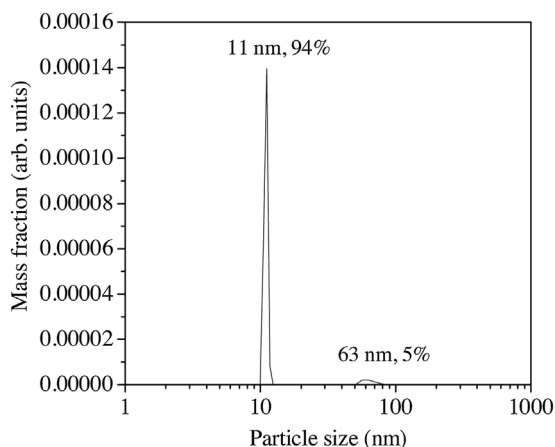
Figure 7 Particle size distribution of boron-doped diamonds (synthesized from 9BBN) in water suspension.

at pressures of 8–9 GPa and temperatures of 970–1400 °C, for nanodiamond formation from 9BBN.

3.4 Aqueous suspensions of boron-doped nanodiamonds Samples, synthesized from 9BBN at temperatures up to 1250–1310 °C, were chemical purified from the non-diamond phases, and aqueous suspensions of purified diamond particles were subsequently prepared.

Raman spectrum of the nanodiamonds obtained after purification (not shown here) is practically the same in the range below 1330 cm^{-1} as for as-synthesized (at 1600 °C) microcrystalline heavily boron-doped diamond (see upper spectrum in Fig. 2c and the sample morphology in Fig. 1c), which implies intake of boron impurity in nanodiamond; boron carbide lines were not detected in Raman spectra of the purified samples. Particle size distribution of boron-doped nanodiamonds in water suspensions measured by dynamic light scattering (DLS) is shown in Fig. 7 for the sample synthesized at 1310 °C: about 94% vol. of nanoparticles have the size of 11 nm and small fraction is around 63 nm. The measured particle size distribution is consistent with corresponding TEM data revealing the appearance of diamond crystals with size of 50 nm at temperatures of 1400 °C. Note that 1250–1400 °C is expected to be a temperature range when diamond nuclei start to grow up in the hydrogen-based growth medium.

4 Summary We studied the behavior of boranes with sp^3- and sp^2-hybridized carbon at the temperature (up to 1600–1700 °C) and pressure (8–9 GPa) treatment. It was shown that the planar structure of carbon cycles in triphenylborane and trimesitylborane induces their transformation into graphite upon HPHT decomposition. In turn, bridged structure of 9BBN molecules and the presence of boron in the carbon cycle lead to the formation of diamond nanocrystals in the temperature range from 970 to 1400 °C. Observed evolution of diamond and graphite phases and changes in diamond crystal sizes with temperature suggest the existence of two mechanisms of the diamond synthesis from 9BBN depending on the temperature range. First mechanism, which realized in the range 970–1400 °C, is the diffusional transformation of the disordered carbon phase into diamond and graphite nanocrystals with the sizes generally below ~10 nm. Second one is a catalytic conversion of graphite into diamond in the range 1400–1700 °C, characterized by the formation of diamond crystals of various sizes, up to a few microns. A water suspension of the boron-doped diamond nanoparticles with a narrow size distribution can be easily prepared from the samples synthesized at 1200–1300 °C, that essentially simplify scientific and technologic application of this material. Conductive nanodiamonds can be used for seeding during the CVD film synthesis without breaking electrical contact with the conductive substrate [6], as a conductive "ink" to create conductive structures [5], for drug delivery in biomedicine, in order to create elements of superconducting devices etc.

References

[1] R. H. Wentorf, J. Phys. Chem. **69**, 3063 (1965).
[2] I. Aharonovich, S. Castelletto, D. A. Simpson, C. H. Su, A. D. Greentree, and S. Prawer, Rep. Prog. Phys. **74**, 076501 (2011).
[3] S. Mandal, C. Naud, O. A. Williams, É. Bustarret, F. Omnès, P. Rodière, T. Meunier, L. Saminadayar, and C. Bäuerle, Nanotechnology **21**, 195303 (2010).
[4] S. Mandal, T. Bautze, O. A. Williams, C. Naud, E. Bustarret, F. Omnes, P. Rodiere, T. Meunier, C. Bauerle, and L. Saminadayar, ACS Nano **5**, 7144 (2011).
[5] T. Kondo, M. Horitani, H. Sakamoto, I. Shitanda, Y. Hoshi, M. Itagaki, and M. Yuasa, Chem. Lett. **42**, 352 (2013).
[6] M. Tsigkourakos, T. Hantschel, D. K. Simon, T. Nuytten, A. S. Verhulst, B. Douhard, and W. Vandervorst, Carbon **79**, 103 (2014).
[7] T. Bautze, S. Mandal, O. A. Williams, P. Rodiere, T. Meunier, and C. Bauerle, Carbon **72**, 100 (2014).
[8] E. A. Ekimov, S. G. Lyapin, K. N. Boldyrev, M. V. Kondrin, R. Khmelnitskiy, V. A. Gavva, T. V. Kotereva, and M. N. Popova, JETP Lett. **102**, 701 (2015).
[9] V. A. Davydov, A. V. Rakhmanina, S. G. Lyapin, I. D. Ilichev, K. N. Boldyrev, A. A. Shiryaev, and V. N. Agafonov, JETP Lett. **99**, 585 (2014).
[10] U. Jantzen, A. B. Kurz, D. S. Rudnicki, C. Schäfermeier, K. D. Jahnke, U. L. Andersen, V. A. Davydov, V. N. Agafonov, A. Kubanek, L. J. Rogers, U. L. Andersen, and F. Jelezko, preprint, arXiv:1602.03391 (2016).
[11] E. A. Ekimov, O. S. Kudryavtsev, A. A. Khomich, O. I. Lebedev, T. A. Dolenko, and I. I. Vlasov, Adv. Mater. **27**, 5518 (2015).
[12] F. P. Bundy, J. Chem. Phys. **38**, 631 (1963).
[13] H. Sumiya, SEI Tech. Rev. **74**, 15 (2012).
[14] A. Onodera, K. Suito, and Y. Morigami, Proc. Jpn. Acad. B **68**, 167 (1992).

[15] A. Onodera and K. Suito, in: Proceedings of AIRAPT-17, Hawaii, USA, 1999 (Universities Press, Hyderabad, India, 2000), pp. 875–880.

[16] V. A. Davydov, A. V. Rakhmanina, V. Agafonov, and V. N. Khabashesku, Carbon **90**, 231 (2015).

[17] C. Le Guillou, F. Brunet, T. Irifune, H. Ohfuji, and J. N. Rouzaud, Carbon **45**, 636 (2007).

[18] E. A. Ekimov, R. A. Sadykov, S. Gierlotka, A. Presz, E. V. Tatyanin, V. N. Slesarev, and N. N. Kuzin, Instrum. Exp. Tech. **47**, 276 (2004).

[19] A. C. Ferrari, Solid State Commun. **143**, 47 (2007).

[20] K. Ushizawa, K. Watanabe, T. Ando, I. Sakaguchi, M. Nishitani-Gamo, Y. Sato, and H. Kanda, Diam. Relat. Mater. **7**, 1719 (1998).

[21] E. A. Ekimov, V. Ralchenko, and A. Popovich, Diam. Relat. Mater. **50**, 15 (2014).

[22] E. A. Ekimov and I. P. Zibrov, Sci. Technol. Adv. Mater. **12**, 055009, (2011).

[23] E. A. Ekimov, I. P. Zibrov, and A. V. Zoteev, Inorg. Mater. **47**, 1194 (2011).

[24] K. Sato and T. Katsura, J. Cryst. Growth **223**, 189 (2001).

[25] S. Yamaoka, M. S. Kumar, M. Akaishi, and H. Kanda, Diam. Relat. Mater. **9**, 1480 (2000).

[26] M. Akaishi, H. Kanda, and S. Yamaoka, Science **259**, 1592 (1993).

[27] M. Akaishi, M. S. Kumar, H. Kanda, and S. Yamaoka, Diam. Relat. Mater. **9**, 1945 (2000).

[28] M. Akaishi and S. Yamaoka, J. Cryst. Growth **209**, 999 (2000).

[29] V. A. Davydov, A. V. Rakhmanina, V. Agafonov, B. Narymbetov, J. P. Boudou, and H. Szwarc, Carbon **42**, 261 (2004).